Earth and Planetary Science Letters 436 (2016) 19–30

Contents lists available at ScienceDirect

Earth and Planetary Science Letters

www.elsevier.com/locate/epsl

Two decades of spatiotemporal variations in subduction zone coupling offshore Japan

John P. Loveless [a,*], Brendan J. Meade [b]

[a] Department of Geosciences, Smith College, 44 College Lane, Northampton, MA 01063, USA
[b] Department of Earth and Planetary Sciences, Harvard University, 20 Oxford Street, Cambridge, MA 02138, USA

A R T I C L E I N F O

Article history:
Received 21 July 2015
Received in revised form 21 December 2015
Accepted 22 December 2015
Available online 7 January 2016
Editor: P. Shearer

Keywords:
subduction zone
Japan
coupling
earthquake cycle

A B S T R A C T

Spatial patterns of interplate coupling on global subduction zones can be used to guide seismic hazard assessment, but estimates of coupling are often constrained using a limited temporal range of geodetic data. Here we analyze ∼19 years of geodetic observations from the GEONET network to assess time-dependent variations in the spatial distribution of coupling on the subduction zones offshore Japan. We divide the position time series into five, ∼3.75-year epochs each decomposed into best-fit velocity, annual periodic signals, coseismic offsets, and postseismic effects following seven major earthquakes. Nominally interseismic velocities are interpreted in terms of a combination of tectonic block motions and earthquake cycle activity. The duration of the inferred postseismic activity covaries with the linear velocity. To address this trade-off, we assume that the nominally interseismic velocity at each station varies minimally from epoch to epoch. This approach is distinct from prior time-series analysis across the earthquake cycle in that position data are not detrended using preseismic velocity, which inherently assumes that interseismic processes are spatially stable through time, but rather the best-fit velocity at each station may vary between epochs. These velocities reveal significant consistency since 1996 in the spatial distribution of coupling on the Nankai subduction zone, with variation limited primarily to the Tokai and Bungo Channel regions, where long-term slow slip events have occurred, and persistently coupled regions coincident with areas that slipped during historic great earthquakes. On the Sagami subduction zone south of Tokyo, we also estimate relatively stable coupling through time. On the Japan–Kuril Trench, we image significant coupling variations owing to effects of the 1994 $M_W = 7.7$ Sanriku-oki, 2003 $M_W = 8.2$ Tokachi-oki, and 2011 $M_W = 9.0$ Tohoku-oki earthquakes. In particular, strong coupling becomes more spatially extensive following the 1994 event until 2011, coseismic-sense slip precedes the Tohoku-oki event, and coupling offshore northern Honshu is reduced after the 2011 earthquake. Despite the occurrence of the 2003 Tokachi-oki earthquake, persistent coupling offshore Hokkaido suggests ongoing seismic hazard, possibly similar to past M_W∼9-class earthquakes interpreted from coastal paleoseismic records. This time-dependent analysis of interseismic deformation illuminates rich diversity in the distribution of subduction zone coupling, including spatiotemporal stability in coupling, effective reduction in strongly coupled regions due to aseismic thrust-sense slip events, and broad changes in the distribution of coupling following major earthquakes.

1. Introduction

Over the past two decades, the proliferation of high-precision geodetic observations and occurrence of large earthquakes have enabled imaging of processes spanning the earthquake cycle, including interseismic strain accumulation, abrupt coseismic strain release, and transient behavior such as postseismic afterslip, postseismic viscoelastic relaxation of the lower crust and/or upper mantle, and aseismic slip during the nominally interseismic period. Geodetic displacement time series have led to the discovery of spatial variations in interseismic coupling (McCaffrey et al., 2000; Nishimura et al., 2004), constraints on the viscosity of Earth's lower crust (Hearn et al., 2009; Pollitz et al., 2000), and the occurrence of aseismic slow slip events (Dragert et al., 2001; Hirose et al., 1999).

The GEONET GNSS array has measured surface displacement across the Japanese Islands at >800 stations since 1996. These

* Corresponding author. Tel.: +1 413 585 2657.
E-mail addresses: jloveless@smith.edu (J.P. Loveless), meade@fas.harvard.edu (B.J. Meade).

http://dx.doi.org/10.1016/j.epsl.2015.12.033

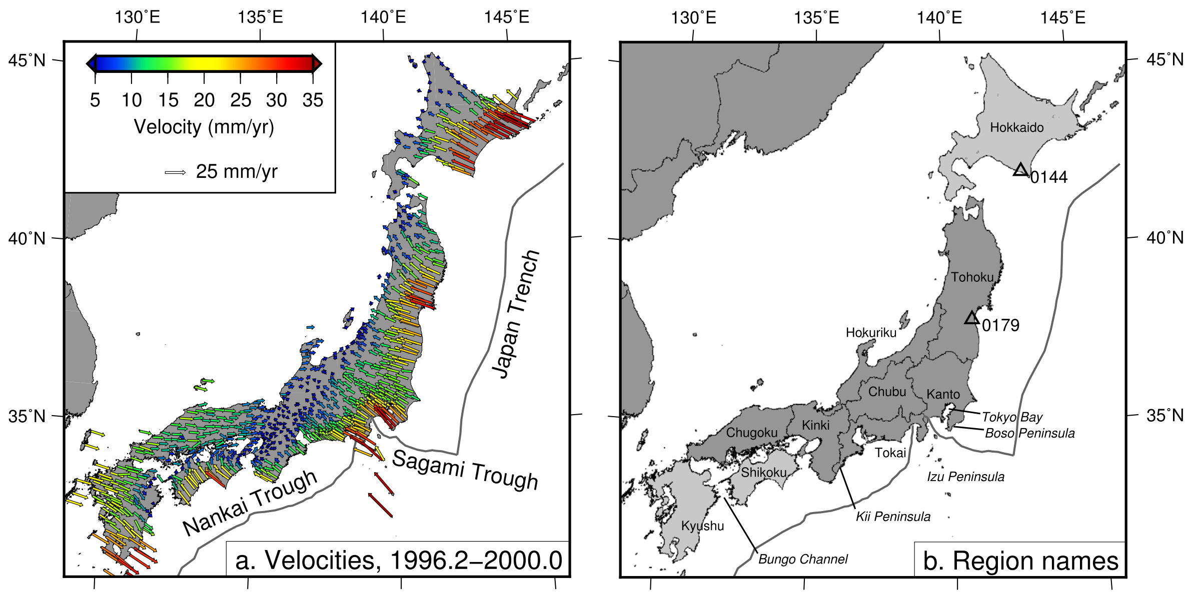

Fig. 1. a) Nominally interseismic velocity field for GEONET stations, April 1, 1996–December 31, 1999, expressed relative to the stable Eurasia reference frame of Apel et al. (2006). b) Regions and localities of Japan referred to in the text. The labeled darker gray regions comprise the island of Honshu. Position time series for stations 0144 and 0179 are shown in Fig. 2.

crustal deformation observations have been interpreted as reflecting earthquake cycle processes on the network of crustal faults throughout Japan and the three subduction interfaces offshore (Nankai Trough, Sagami Trough, Japan–Kuril Trench; Fig. 1a) (Hashimoto et al., 2000; Loveless and Meade, 2010; Nishimura et al., 2004). Previous studies have focused on either spatiotemporal evolution of subduction zone coupling on an isolated subduction zone section (Hashimoto et al., 2009; Liu et al., 2010; Mavrommatis et al., 2014; Nishimura et al., 2004), or nationwide tectonics using a limited time period of GEONET observations (Hashimoto et al., 2000; Loveless and Meade, 2010).

Here we analyze GEONET data in five, ∼3.75-year epochs spanning April 1996 through December 2014. For each epoch, we fit each station time series with a combination of linear, periodic, step, and exponential functions, which we interpret to represent nominally interseismic deformation related to earthquake cycle processes on the subduction zones and crustal faults, seasonal effects, offsets due to earthquakes and equipment maintenance, and postseismic deformation following large earthquakes, respectively. We use the linear velocity fields as constraints on quasi-static elastic block models, which provide a means for interpreting geodetic observations resulting from the combined effects of tectonic block rotations, earthquake cycle processes (Meade and Loveless, 2009), and volume changes of magma bodies. We use these models to image patterns of subduction zone coupling in each of the five epochs, identifying persistently coupled regions, effects of large earthquakes on subduction zone coupling, and the occurrence of aseismic slip events.

2. Methods

2.1. Decomposition of displacement time series

We analyze F3 daily coordinates from the Geospatial Information Authority of Japan during five time periods: April 1, 1996–December 31, 1999 (1996.25–2000.00; 3.75 year duration); January 1, 2000–September 24, 2003 (before the $M_W = 8.2$ Tokachi-oki earthquake offshore Hokkaido, 2000.00–2003.73; 3.73 years); September 25, 2003–June 30, 2007 (2003.73–2007.50; 3.77 years); July 1, 2007–March 10, 2011 (before the $M_W = 9.0$ Tohoku-oki earthquake offshore northern Honshu, 2007.50–2011.19; 3.69 years); and March 11, 2011–December 31, 2014 (2011.19–2015.00; 3.81 years). For the entire time series, we fit individual station position time series, $\mathbf{x}(t)$, where the vector $\mathbf{x}$ represents the position in the east or north direction, using piecewise linear, periodic, step and exponential functions:

$$\mathbf{x}(t) = \sum_{i=1}^{N_{\text{epoch}}} \mathbf{A}_i * I(t-t_i) + \sum_{j=1}^{2}\left(\mathbf{B}_j \sin\frac{2\pi jt}{T_{\text{yr}}} + \mathbf{C}_j \cos\frac{2\pi jt}{T_{\text{yr}}}\right) + \sum_{k=1}^{N_{\text{step}}} \mathbf{D}_k \text{H}(t-t_k) + \sum_{m=1}^{2}\sum_{n=1}^{N_{\text{eq}}} \mathbf{E}_{(2(n-1)+m)} \text{H}(t-t_n)\left(1-e^{(t_n-t)/\tau_m}\right), \tag{1a}$$

where

$$I = \begin{cases} 1 & \text{for } t_i \le t < t_{i+1} \\ 0 & \text{for } t < t_i \text{ and } t \ge t_{i+1} \end{cases}, \tag{1b}$$

and

$$\tau_m = \frac{P_m * T_{\text{yr}}}{-\ln(0.05)}. \tag{1c}$$

A is the linear slope during each epoch, which we take to reflect the nominally interseismic velocity; I is an index function defined such that $I = 1$ for time values within the epoch and zero for times before and after; **B** and **C** are amplitudes of annual and semiannual periodic terms; **D** gives the amplitude of steps in the time series corresponding to earthquakes, equipment (antenna) changes, and ordinate-intercepts accompanying linear terms; H is the Heaviside step function; and **E** is the amplitude of postseismic deformation following specified earthquakes. The decay constants, τ_m, correspond to durations P_m (in years) following an earthquake when the exponential function reaches 95% peak asymptotic amplitude **E**. In all terms, t is the time in days since the beginning of the analysis time period, T_{yr} is the duration of a year in days, and subscripted t values in linear, step, and exponential functions refer to dates of epoch initiation, offsets, and major earthquakes, respectively. We consider 23 values of τ_2, corresponding to durations of exponential signal ranging from 6 months to 10 years